MATEC Web of Conferences **1**, 08001 (2012)
DOI: 10.1051/matecconf/20120108001

Bifurcation of Contact Between Rotor and Stator

Oliver Alber[1,a] and Richard Markert[1]

Structural Dynamics, Darmstadt University of Technology, Petersenstr. 30, 64287 Darmstadt, Germany

Abstract. The paper discusses Bifurcation Diagrams of rotor stator contact problems and the transition from synchronous whirl towards different asynchronous movement patterns. Bifurcation Diagrams based on Poincaré Maps are presented for the model consisting of a Jeffcott rotor and a flexible mounted rigid stator ring. The analysis methods are applied systematically with respect to various motion patterns that have been observed for rotor stator contact in the past. The type of motion is identified using the analysis methods. Also the influence of different parameters on the changes of motion patterns and the transitions that result are described. The unique identification of all motion patterns for rotor stator interaction based on Bifurcation Diagrams is focus of the paper. Further insight on the conditions that lead to the change of motion patterns is given.

1 Introduction and Motivation

When an rotor contacts a non-rotating part (e.g. the housing), the system becomes non-linear and various motion patterns are possible. Depending on the initial conditions, different motion patterns may develop for the same parameter set, e.g. in figure 1 at rotor speed $\Omega = 0.84\,\omega_R$ forward or backward whirl motion arise. The regular unbalance response is the synchronous motion. If however the synchronous motion is unstable (e.g. dashed line in figure 1), asynchronous motion occur. These include forward or backward whirl, sub- or super-harmonic vibrations, motion with sidebands around the synchronous motion or even chaotic motion [1]. Asynchronous motion patterns (especially in the case of backward whirl) may exhibit large vibration amplitudes combined with huge contact forces that might lead to severe damage of the rotor stator system.

Bifurcation Diagrams give rise to the behavior of motion states during modification of system parameters. Many publications discussing bifurcation in rotor stator interaction problems can be found with different modeling assumptions. Most of them are using either a rigidly mounted stator (referred as *Rub Impact*) or a massless stator, which is not capable to model systems with significant stator mass. Popprath and Ecker [2] include mass effects, but focus on periodic, multi-periodic and chaotic motions. Forward and backward whirl are not included and Bifurcation Diagrams are only available for the variation of rotation speed and mass ratio. However for technical systems in operation, a change of the friction in the contact surfaces is more likely than a change of rotor and stator mass ratio. Despite that, all investigations of literature detected the friction coefficient as the major determining parameter for asynchronous motion. Especially forward and backward whirl motion are quite sensitive to the friction coefficient whereas subharmonic motion is generated by stator offset [3].

This paper shows how each motion pattern of rotor stator interaction can be uniquely identified in Bifurcation Diagrams and Poincaré Maps and studies their dependence from relevant parameters.

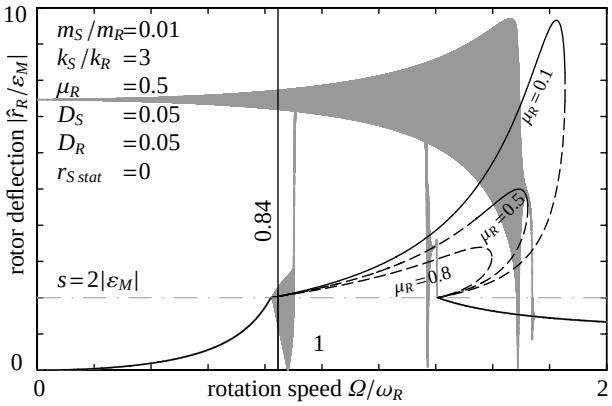

Fig. 1: Unbalance response of a Jeffcott rotor contacting the stator for $\mu_R = 0.5$; analytical solution for different values of μ_R

2 Model and Analysis Methods

The model investigated consists of a Jeffcott rotor with

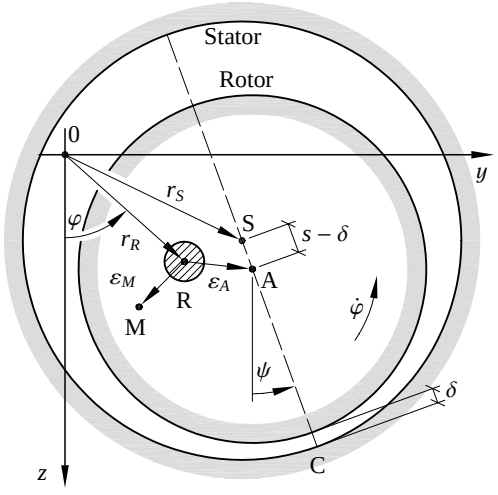

Fig. 2: Kinematics of rotor and stator [1]

[a] e-mail: alber@sdy.tu-darmstadt.de

mass m_R, stiffness k_R and mass excentricity ε_M and a flexible mounted rigid stator with mass m_S and mounting stiffness k_S. Both, rotor and stator account for external viscous damping (D_S, D_R) and may account for a stator offset $r_{S\,stat}$. The contact areas of rotor and stator are cylindrical surfaces with an average clearance s. The kinematic relation between s, r_R, r_S, rotor to stator distance δ and the direction ψ of the contact force shown in figure 2 is described by

$$r_R - r_S = (s-\delta)e^{i\psi} \tag{1}$$

using complex notation. The contact force F_C is described by a pseudo-linear viscoelastic contact element with contact stiffness k_C, contact damping b_C and friction coefficient μ_R,

$$F_C = (1+i\mu_R)\left\langle -k_C\delta - b_C\langle\dot{\delta}\rangle\right\rangle\langle-\delta\rangle^0 e^{i\psi}, \tag{2}$$

where $\langle x\rangle = x$ only for $x > 0$. This simple model includes all effects for replicating the various motion patterns mentioned above [3]. The equations of motion for rotor and stator displacement r_R and r_S are

$$m_R\ddot{r}_R + b_R\dot{r}_R + k_R r_R = -m_R\varepsilon_M(e^{i\varphi})^{\cdot\cdot} - F_C \tag{3}$$

$$m_S\ddot{r}_S + b_S\dot{r}_S + k_S(r_S - r_{S\,stat}) = F_C. \tag{4}$$

Poincaré Maps for forced vibration systems can be used to identify periodic or quasi-periodic as well as chaotic motion. To differ between quasi-periodic and chaotic motion the phase-plane Poincaré Map or the frequency spectrum has to be studied additionally [4]. If the Poincaré Maps are used as a base for Bifurcation Diagrams, it is possible to study the effect of parameter changes on different motion states of non-linear systems. For sampling at fixed rotation angle positions with sampling times

$$t_n = n\frac{2\pi}{\Omega} + \tau_0 \tag{5}$$

according to [4] the Poincaré Maps in phase-plane look as follows:

- Synchronous motion (periodic motion): One point
- Subharmonic motion n-th order (period-n-motion): n points
- Quasi-periodic motion with two incomensurate frequencies: Closed curve
- Quasi-periodic motion with more than two dominant incommensurable frequencies, chaotic motion: Fuzzy collection of points

To construct the full spectrum of motion patterns different initial conditions are used which are chosen individually from observations of quasi-stationary runups and rundowns. Also analytical solutions for synchronous motion (as well as its stability) and for backward whirl according to [1] are used as initial states. This analytical previous knowledge is displayed for better understanding as black lines in the Bifurcation Diagrams.

3 Forward and Backward Whirl

Beside the synchronous motion forward and backward whirl are possible at the same rotor speed. This situation is shown in figure 1 at rotor speed $\Omega = 0.84\omega_R$. The corresponding Bifurcation Diagram is shown in figure 3. Figure 3 shows also corresponding orbits, phase-planes and spectra for different friction coefficients μ_R.

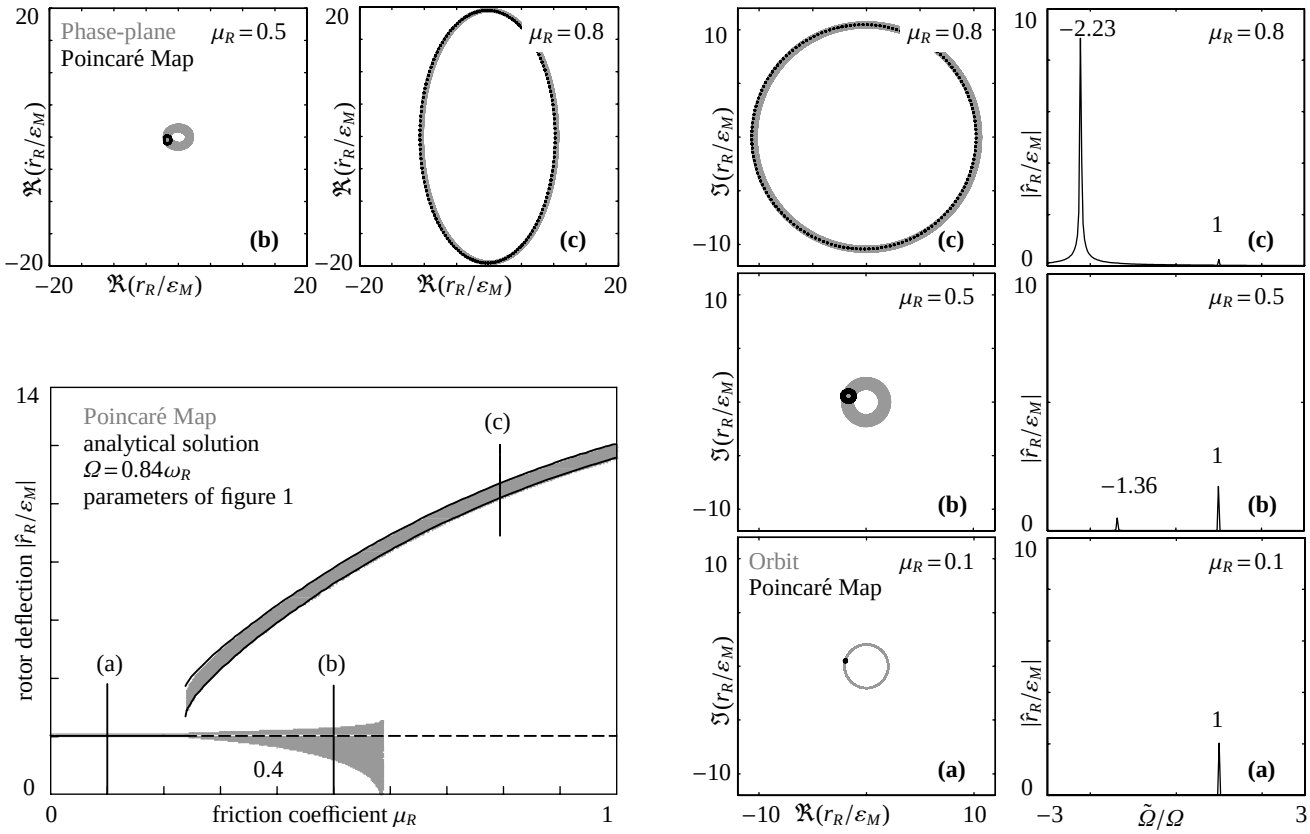

Fig. 3: Bifurcation Diagram, spectra, orbits and phase-planes for variation of μ_R for parameters of figure 1 at rotor speed $\Omega = 0.84\omega_R$

The grey points show the Bifurcation Diagram for the variation of the friction coefficient μ_R. For low friction (a) the synchronous unbalance response is stable, no forward or backward whirl exist. As the friction coefficient increases, the synchronous motion becomes unstable and asynchronous motion patterns occur. In the lower branch forward whirl develops (b) until the rotor deflection amplitude reaches the value zero. In the same range of μ_R in which forward whirl exists, backward whirl coexists in the upper branch. For large μ_R backward whirl with large increasing rotor deflection is the only motion pattern (c). Both, forward and backward whirl are represented as sharply limited bands in the Bifurcation Diagram, synchronous motion as a straight line. In this regime the approximate analytical solution of backward whirl (thin solid black line, see [1]) is a good approximation for the real behavior. At the transition from synchronous motion to backward whirl the rotor deflection changes abruptly as μ_R is increased. This sudden change is more dangerous for a running rotor contacting the stator than the smooth change during transition from synchronous motion to forward whirl in the lower branch. As expected, the points obtained by the Poincaré Map in orbits and phase-planes form closed curves. The Poincaré Mapping points of backward whirl surround the rotor center of the orbit. For forward whirl the points surround only the point of the synchronous motion, as the synchronous frequency component is dominant.

4 Subharmonic Oscillations

Subharmonic motion arises if the stator is misaligned to the rotor. Such a behavior is shown in figure 4. The unbalance response includes subharmonics in the resonance speed range but more evident at speed around $\Omega = 2.6\,\omega_R$. Figure 5 shows the corresponding Bifurcation Diagram, spectrum, orbit and phase-plane. Obviously, the stator offset $r_{S\,stat}$ contributes significantly to the development of subharmonic motion of second order. Transition from synchronous to subharmonic motion (Pitchfork Bifurcation) occurs when the stator offset exceeds a certain value. At the transition point a jump of the rotor deflection occurs. If the stator offset is beyond a critical value, the subharmonic motion again becomes a synchronous motion. As expected, subharmonic motion of order two produces two points for the Poincaré Map in orbit and phase-plane.

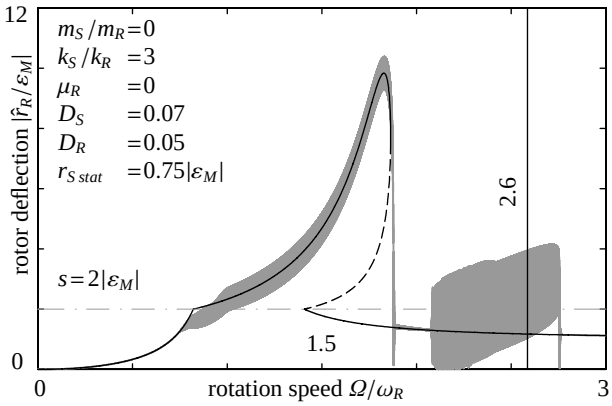

Fig. 4: Unbalance response at stator misalignment $r_{S\,stat}$

5 Superharmonics, Chaotics and Sidebands

Rotor stator systems, where the lowest rotor eigenfrequency is higher than the stator eigenfrequency, show a complex, but also very interesting dynamic behavior. Such a behavior is exemplarily shown in figure 6 for a particular parameter set. Beside the trivial contact-free and the non-trivial contact-afflicted synchronous motion superharmonic oscillations, backward whirl, nearly synchronous motions with sidebands and even chaotic oscillations show up.

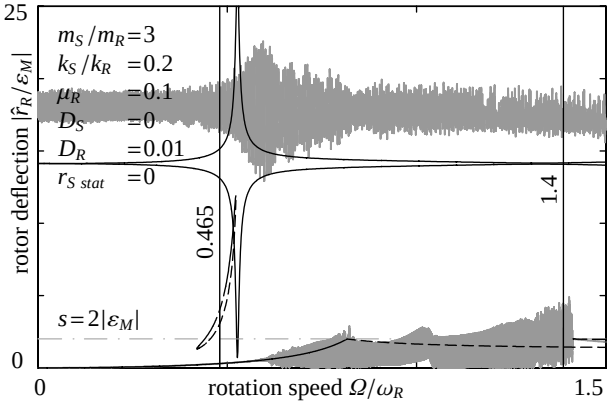

Fig. 6: Unbalance response of a rotor with heavy stator

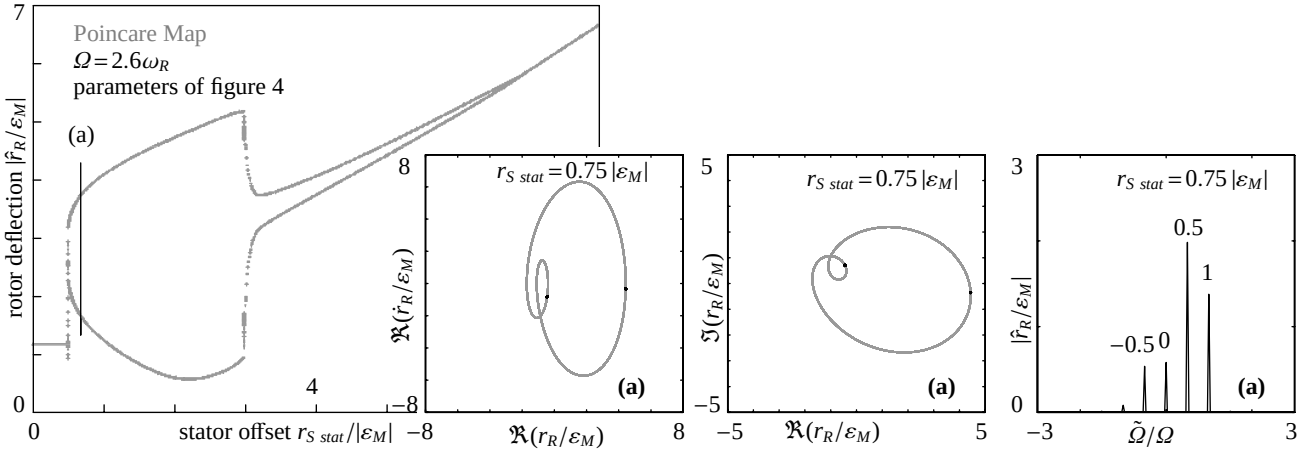

Fig. 5: Bifurcation Diagram, spectrum, orbit and phase-plane for variation of $r_{S\,stat}$ for parameters of figure 4 at rotor speed $\Omega=2.6\omega_R$

Figure 7 shows Bifurcation Diagram, spectrum, orbit and phase-plane at rotor speed of $\Omega = 0.465\,\omega_R$ depending on the friction coefficient. The lowest line (1) represents the motion without contact between rotor and stator. Parallel to this line exists the synchronous motion with contact with an unstable lower branch (2) and a partially stable upper branch (3). The synchronous motion on the upper branch (3) smoothly evolves into a superharmonic motion (a) by increasing μ_R. Previous analytical stability investigations of synchronous motion [1] are not able to predict the transition point exactly, but give a certain indication for asynchronous motions. If μ_R is increased further, the superharmonic motion decays and only synchronous motion without contact or backward whirl is possible. The analytical approximation for the backward amplitude developed in [1] deviates with rising friction coefficient more and more from the Poincaré points. This is originated in the increasing additional multi-frequent components contained in the oscillation signal which are neglected in analysis. The points obtained by the Poincaré Map in orbit and phase-plane of the superharmonic motion form closed curves. Beside the friction coefficient μ_R the rotor damping is a parameter with strong impact. Figure 8 shows the Bifurcation Diagram and corresponding spectra, orbits and phase-planes at rotor speed of $\Omega = 1.4\,\omega_R$ depending on the damping ratio $D_R = b_R/(2\sqrt{k_R m_R})$. For low damping chaotic vibrations exist (a): Phase-plane and orbit show no regular patterns and random frequencies are present in a wide band of the spectrum. At high rotor amplitude also a backward whirl motion is present for low damping D_R. With increasing D_R the chaotic motion converts to a motion with sidebands around the synchronous component. At about $D_R = 0.34$ a stable synchronous motion exists, but becomes unstable with increasing D_R and motion with sidebands occur (b). For this motion the Poincaré Maps in orbit and phase-plane are closed curves and the noise in the spectrum disappears. It can be concluded that for the special parameters used a low damping ratio supports chaotic vibrations. For a high damping ratio sideband vibrations may occur even if the synchronous motion without contact exists.

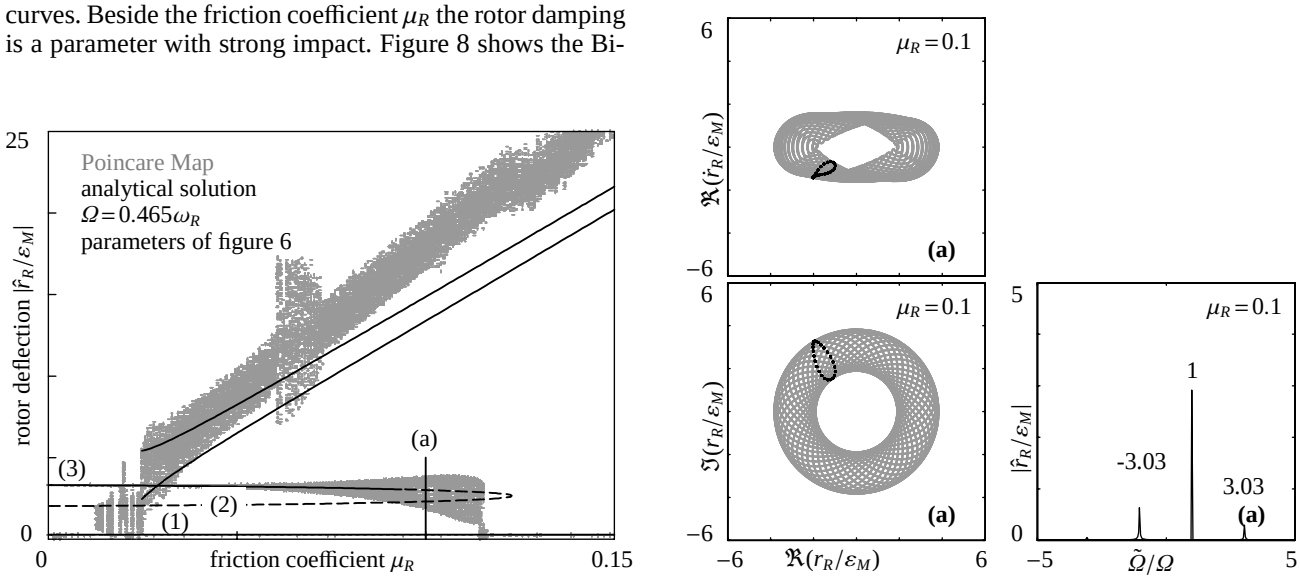

Fig. 7: Bifurcation Diagram, spectrum, orbit and phase-plane for variation of μ_R for parameters of figure 6 at rotor speed $\Omega = 0.465\omega_R$

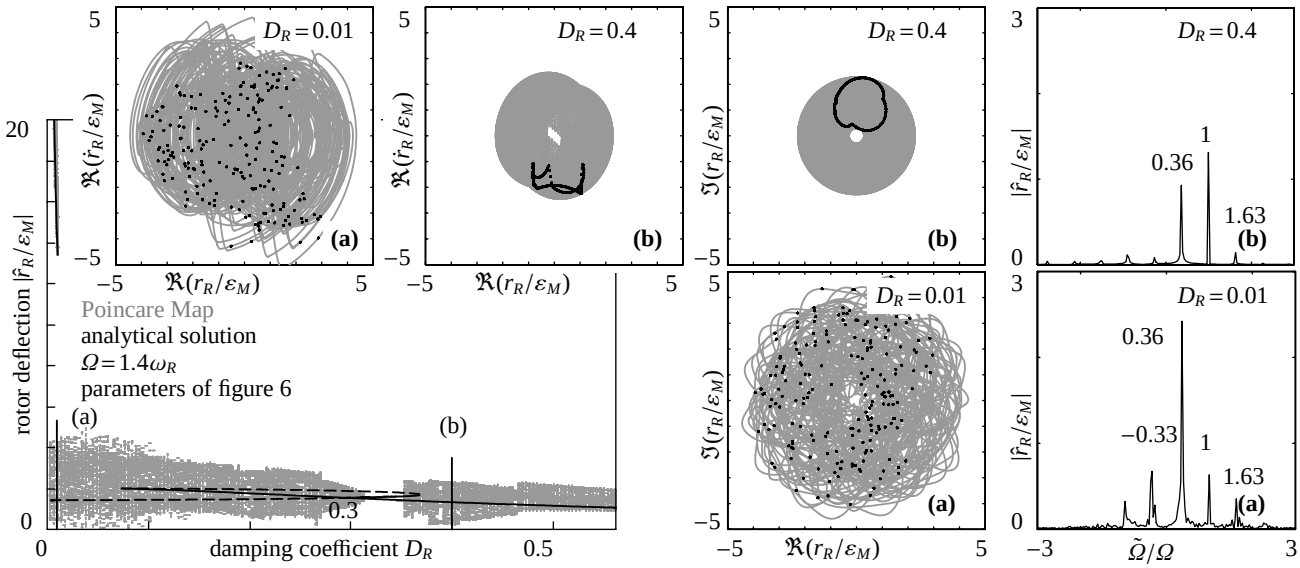

Fig. 8: Bifurcation Diagram, spectra, orbits and phase-planes for variation of D_R for parameters of figure 6 at rotor speed $\Omega = 1.4\omega_R$

6 Conclusion

Bifurcation Diagrams are able to summarize the effects of parameter changes on state variables directly, which is very useful for investigating systems endangered to rub. For whirl motion (figure 3) it is necessary to choose the correct state variable to be displayed in the Bifurcation Diagram. Displaying the rotor deflection in one direction only, which is predominantly done in former studies [2], to distinguish between coexisting backward and forward whirl is impossible, because in the Bifurcation Diagram forward and backward whirl are overlayed by each other. Using amplitudes of rotor or stator displacement or contact force is more suitable. The shapes of orbits and the position of Poincar'e Mapping points in the orbits are similar to that of the phase-planes, therefore it is sufficient to display either orbits or phase-planes for solely determinating the motion states. For the presented Bifurcation Diagrams and Poincaré Maps a unique identification of synchronous, subharmonic and chaotic motion is possible. Bifurcation analysis is not able to distinguish between forward and backward whirl, superharmonic motion and sideband motion around the synchronous motion. Beside Bifurcation Diagrams and phase-planes spectra [3] are helpful.

References

1. U. Ehehalt,: *Bewegungsformen elastischer Rotoren bei Statorkontakt* (Fortschritt-Berichte VDI Reihe 11 Nr. 335, 2008)
2. S. Popprath, H. Ecker: Nonlinear dynamics of a rotor contacting an elastically suspended stator; Journal of Sound and Vibration **308**, (2007) 767-784
3. U. Ehehalt, E. Hahn, R. Markert: Motion Patterns at Rotor Stator Contact; *ASME Conference Proceedings* (ASME, 2005) 1031-1042
4. F. C. Moon, *Chaotic Vibrations* (John Wiley & Sons, New York 1987)